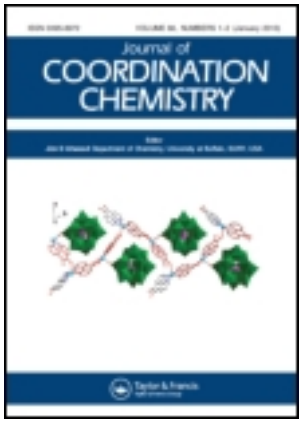

Journal of Coordination Chemistry
Publication details, including instructions for authors and subscription information:
http://www.tandfonline.com/loi/gcoo20

A new organopolymolybdate polymer for linking metal-organic moiety through Mo-N bonds

Ai-Xiang Tian [a] , Xiao-Ling Lin [a] , Gui-Ying Liu [b] , Ru Xiao [a] , Jun Ying [a] & Xiu-Li Wang [a]

[a] Department of Chemistry , Bohai University , Jinzhou , P.R. China

[b] Liaoning Ocean and Fisheries Science Research Institute , DaLian , P.R. China

Accepted author version posted online: 05 Mar 2013.Published online: 09 Apr 2013.

To cite this article: Ai-Xiang Tian , Xiao-Ling Lin , Gui-Ying Liu , Ru Xiao , Jun Ying & Xiu-Li Wang (2013) A new organopolymolybdate polymer for linking metal-organic moiety through Mo-N bonds, Journal of Coordination Chemistry, 66:8, 1340-1349, DOI: 10.1080/00958972.2013.780204

To link to this article: http://dx.doi.org/10.1080/00958972.2013.780204

Journal of Coordination Chemistry, 2013
Vol. 66, No. 8, 1340–1349, http://dx.doi.org/10.1080/00958972.2013.780204

A new organopolymolybdate polymer for linking metal-organic moiety through Mo–N bonds

AI-XIANG TIAN†*, XIAO-LING LIN†, GUI-YING LIU‡, RU XIAO†, JUN YING† and XIU-LI WANG†

†Department of Chemistry, Bohai University, Jinzhou, P.R. China;
‡Liaoning Ocean and Fisheries Science Research Institute, DaLian, P.R. China

(*Received 21 May 2012; in final form 12 December 2012*)

A new organopolymolybdate polymer, $[Zn_2(H_2biim)_4(Hbiim)_2][H_2(\gamma\text{-}Mo_8O_{26})]\cdot 8H_2O$ (**1**) (H_2biim = 2,2′–biimidazole), was synthesized under hydrothermal conditions. In **1**, H_2biim has chelate and linking roles. Three H_2biim chelate one Zn to form a cationic metal-organic subunit; two subunits link one octamolybdate through Mo–N bonds, forming a two-supporting anion. There are abundant $\pi\ldots\pi$ stacking interactions between these anions inducing a 1-D supramolecular chain. The electrochemical behavior and photoluminescence of **1** have been studied.

Keywords: Polyoxometalate; Octamolybdate; Mo–N bond; Electrochemical property; Photoluminescence

1. Introduction

Polyoxometalates (POMs), as a unique class of metal-oxide clusters, exhibit structural diversity [1] and own various physical and chemical properties, such as catalytic, electrochemical and photochemical activities; ion exchange; and reversible redox behaviors [2]. Introduction of transition-metal complexes (TMCs) to POMs provides a route to construct new frameworks with improved properties [3]. These TMC-modified structures are almost based on Keggin anions [4]. The isopolyanions, such as octamolybdates, are rarely studied [5]. Octamolybdates possess eight isomers, α, β, γ, δ, ε, ξ, θ and η [6], which makes octamolybdate attractive to build new frameworks linked by different TMCs. In these TMC-modified octamolybdate-based compounds, octamolybdates have terminal and bridging oxygens to link metal ions of TMCs through metal–O bonds, inducing a series of high dimensional frameworks [7]. For example, a series of Mo_8-based structures modified by TMCs have been obtained [8]. However, the octamolybdates also can contribute Mo to connect the TMC subunits through Mo–N bonds [9] with N donors provided by organic ligands in TMCs. There are some reports on linking of Mo–N bonds [10]. Thus, exploring the Mo–N linking modes instead of metal–O bonds is a new challenge for isopolymolybdates.

*Corresponding author. Email: tianax717@163.com

The key factor for obtaining TMC-modified octamolybdate compounds containing Mo–N bonds rests on the selection of proper organic ligands. Organic ligands for the construction of this series are based on flexible N-donors in previous reports [11]. Here, we explore new organic ligands to directly link with octamolybdates through Mo–N bonds. Rigid 2,2′–biimidazole (H_2biim) is chosen, which has: (1) four N donors for enhancing coordination; (2) the dispersion of four N donors conducive to coordinate with TM, and Mo. A Mo–N-containing structure was obtained by using H_2biim, $[Zn_2(H_2biim)_4(Hbiim)_2][H_2(\gamma\text{-}Mo_8O_{26})]\cdot 8H_2O$ (**1**). Two cationic metal-organic subunits $[Zn(H_2biim)_2(Hbiim)]^+$ link one octamolybdate through Mo–N bonds, forming a two-supporting anion. In **1**, H_2biim chelates and links.

2. Experimental

2.1. *Materials and methods*

All reagents were of reagent grade and used as received from commercial sources. Elemental analyses (C, H, and N) were performed on a Perkin-Elmer 2400 CHN elemental analyzer. IR spectrum was obtained on an Alpha Centaurt FT/IR spectrometer with KBr pellets from 400–4000 cm^{-1}. The thermal gravimetric analysis (TGA) was carried out under N_2 on a Perkin-Elmer DTA 1700 differential thermal analyzer with a rate of 10.0 °C min^{-1}. Fluorescence spectrum was obtained on an F-4500 spectrofluorometer equipped with a 450 W xenon lamp as the excitation source. Electrochemical measurements were performed with a CHI 660b electrochemical workstation wherea conventional three-electrode system was used. The working electrode was a modified carbon paste electrode (CPE). Ag/AgCl (3 M KCl) electrode was used as a reference electrode and a Pt wire as a counter electrode.

2.2. *Synthesis of $[Zn_2(H_2biim)_4(Hbiim)_2][H_2(\gamma\text{-}Mo_8O_{26})]\cdot 8H_2O$ (1)*

A mixture of $Na_2MoO_4\cdot 2H_2O$ (0.25 g, 1.0 mM), $Zn(CH_3COO)_2\cdot 2H_2O$ (0.22 g, 1.0 mM) and Hbiim (0.067 g, 0.5 mM) was dissolved in 10 mL of distilled water at room temperature. When the pH of the mixture was adjusted to 4.5 with 1.0 M L^{-1} HCl, the suspension was put into a Teflon-lined autoclave and kept under autogenous pressure at 160 °C for 3 days. After slowly cooling to room temperature (final pH = 4.79), light green block crystals were filtered and washed with distilled water (40% yield based on Mo). Anal. Calcd for $C_{36}H_{50}Mo_8N_{24}O_{34}Zn_2$ (2261): C, 19.12; H, 2.23; N, 14.87%. Found: C, 19.16; H, 2.20; N, 14.92%.

2.3. *X-ray crystallography*

Single crystal of **1** with dimensions $0.16 \times 0.14 \times 0.10$ mm was glued on a glass fiber. Data were collected on a CCD diffractometer with graphite-monochromated Mo–K_α radiation ($\lambda = 0.71703$ Å) at 273 K. The structure was refined by full-matrix least-squares on F^2 using the SHELXTL crystallographic software package [12]. Anisotropic thermal parameters were used to refine all non-hydrogen atoms. All hydrogens attached to carbons were generated geometrically, while hydrogens attached to water were not located but were included in the structure factor calculations. The crystal data and structure refinement for **1** are summarized in table 1. Selected bond lengths (Å) and angles (°) are listed in table 2. Crystallographic Data Center with CCDC Number is 870,091 for **1**.

Table 1. Crystal data and structure refinement for **1**.

Formula	$C_{36}H_{50}Mo_8N_{24}O_{34}Zn_2$
*F*w	2261
T (K)	273(2)
Space group	$P2_1/c$
a (Å)	12.6769(7)
b (Å)	15.2167(9)
c (Å)	16.7263(9)
β (°)	94.9600(10)
V (Å^3)	3214.4(3)
Z	2
D_c (g cm^{-3})	2.320
μ (mm^{-1})	2.348
F(0 0 0)	2172
Final $R_1{}^a$, $wR_2{}^b$ [$I > 2\sigma(I)$]	0.0365, 0.1037
Final $R_1{}^a$, $wR_2{}^b$ (all data)	0.0412, 0.1080
GOF on F^2	1.015
Largest diff. peak and holes (e Å^3)	1.626 and −1.588

Table 2. Selected bond lengths (Å) and angles (°) for **1**.

Zn(1)–N(5)	1.911(4)	Zn(1)–N(7)	1.913(4)
Zn(1)–N(3)	1.927(4)	Zn(1)–N(9)	1.934(4)
Zn(1)–N(1)	1.931(4)	Zn(1)–N(11)	1.934(4)
Mo(2)–N(8)	2.206(4)	O(6)–Mo(2)–N(8)	85.65(15)
O(7)–Mo(2)–N(8)	90.59(15)	O(11)–Mo(2)–N(8)	161.11(15)
O(12)–Mo(2)–N(8)	82.04(13)	O(10)–Mo(2)–N(8)	83.20(14)
N(5)–Zn(1)–N(7)	82.42(17)	N(5)–Zn(1)–N(3)	93.65(18)
N(7)–Zn(1)–N(3)	171.95(17)	N(5)–Zn(1)–N(9)	172.63(18)
N(7)–Zn(1)–N(9)	93.64(18)	N(3)–Zn(1)–N(9)	91.00(18)
N(5)–Zn(1)–N(1)	89.75(19)	N(7)–Zn(1)–N(1)	91.01(17)
N(3)–Zn(1)–N(1)	81.92(17)	N(9)–Zn(1)–N(1)	96.57(19)
N(5)–Zn(1)–N(11)	91.90(19)	N(7)–Zn(1)–N(11)	94.60(17)
N(3)–Zn(1)–N(11)	92.55(17)	N(9)–Zn(1)–N(11)	82.18(19)
N(1)–Zn(1)–N(11)	174.32(17)		

Symmetry codes: #1 $-x+3$, $-y+1$, $-z+1$.

2.4. *Preparation of 1–CPE*

Compound **1**-modified CPE (**1**–CPE) was fabricated as follows: 75 mg of graphite powder and 6 mg of **1** were mixed and ground together by an agate mortar and pestle to achieve a uniform mixture, and then 0.1 mL of Nujol was added with stirring. The homogenized mixture was packed into a glass tube with a 1.5 mm inner diameter, and the tube surface was wiped with paper. Electrical contact was established with a copper rod through the back of the electrode.

3. Results and discussion

3.1. *Synthesis*

Hydrothermal technique has proved as an effective method for the preparation of POM-based compounds modified by TMCs [13]. Many factors influence the final structures under hydrothermal conditions, such as crystallization temperature and time, pH, filling volume, *etc.* [14]. Parallel experiments showed that pH was crucial for the synthesis of **1**.

We tried to extend the range of pH (pH > 5 and pH < 3.5), but only pasty suspension was obtained and no crystals were observed. The optimal reaction time and temperature are 3d and 160 °C. If the reaction time is more or less than 3d, although **1** can be still obtained, the yield is lower. Between 140 and180 °C, the yield is highest at 160 °C. When the reaction temperature is higher than 180 °C or lower than 140 °C, no crystals were obtained. In the experimental process, we tried to turn off the drying oven, cooling from 160 °C to room temperature directly. However, the crystal form is rather poor for X-ray diffraction analysis. Thus, we adopted the method of cooling the oven at the rate of 10 °C h^{-1} from 160 to120 °C, and 5 °C h^{-1} from 120 to 80°C and then the oven was turned off. Perfect block crystals were obtained by this method.

3.2. *Description of the structure*

Crystal structure analysis reveals that **1** consists of two Zn^{II} ions, six H_2biim, one $[H_2(\gamma\text{-}Mo_8O_{26})]^{2-}$ (abbreviated to γ-Mo_8), and eight water molcules (figure 1). The γ-Mo_8 is the inorganic building block in **1**, including two $[MoO_5]$ and six $[MoO_6]$ units. The Mo–O bond distances are in the normal ranges [15]. Bond valence sum calculations [16] show that all Mo are + VI and Zn are + II in **1**.

In **1**, there is one crystallographically independent Zn1, six-coordinate by six nitrogens from three H_2biim. The bond distances and angles around Zn1 are 1.911(4)–1.934(4) Å for Zn–N and 81.92(17)–174.32(17) Å for N–Zn–N. The angles and bond distances of Zn in **1** are similar to those in six-coordinate Zn^{II} complexes [17]. Each H_2biim, including N1-, N5- and N9- containing ligands, offers two N donors to chelate Zn. A cationic metal-organic subunit $[Zn(H_2biim)_2(Hbiim)]^+$ is constructed. The N5-containing H_2biim in this $[Zn(H_2biim)_2(Hbiim)]^+$ unit provides N8 donor to connect with Mo2 of a γ-Mo_8 anion. Thus, the N5-containing H_2biim ligand exhibits another linking role. One γ-Mo_8 connects two cationic metal-organic subunits through two Mo2–N8 bonds; the γ-Mo_8 is a two-supporting anion. H_2biim has two roles, chelate and linker, as shown in figure 2. The two $[MoO_5]$ units in γ-Mo_8 form Mo–N bonds in order to satisfy six-coordination of Mo.

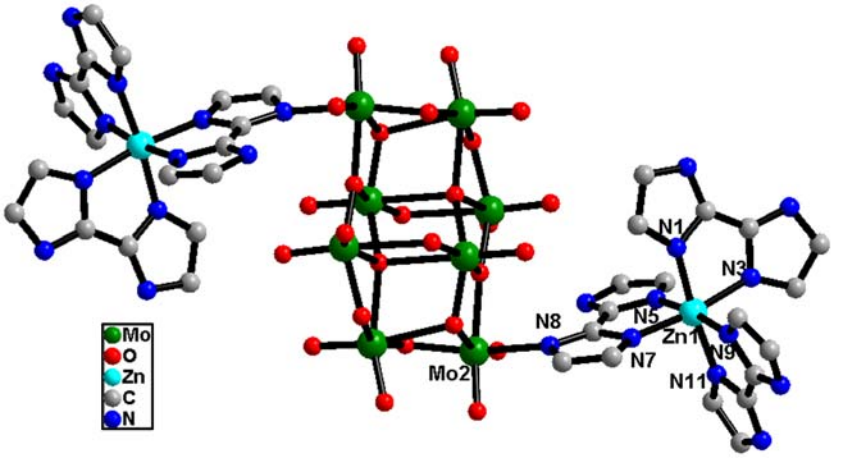

Figure 1. Ball/stick view of the unit of **1**. Hydrogens and waters are omitted for clarity.

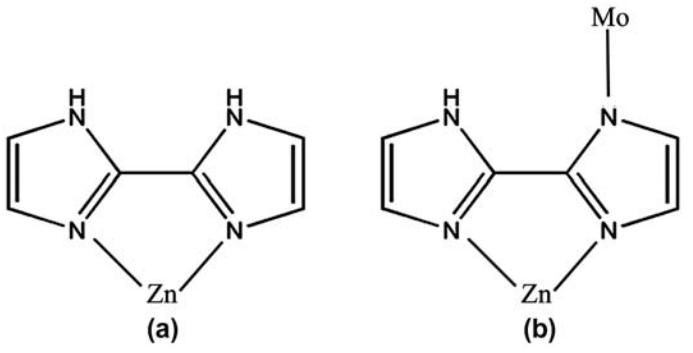

Figure 2. Two coordination modes of H_2biim, acting as chelate and linking through Zn-N and Mo–N bonds.

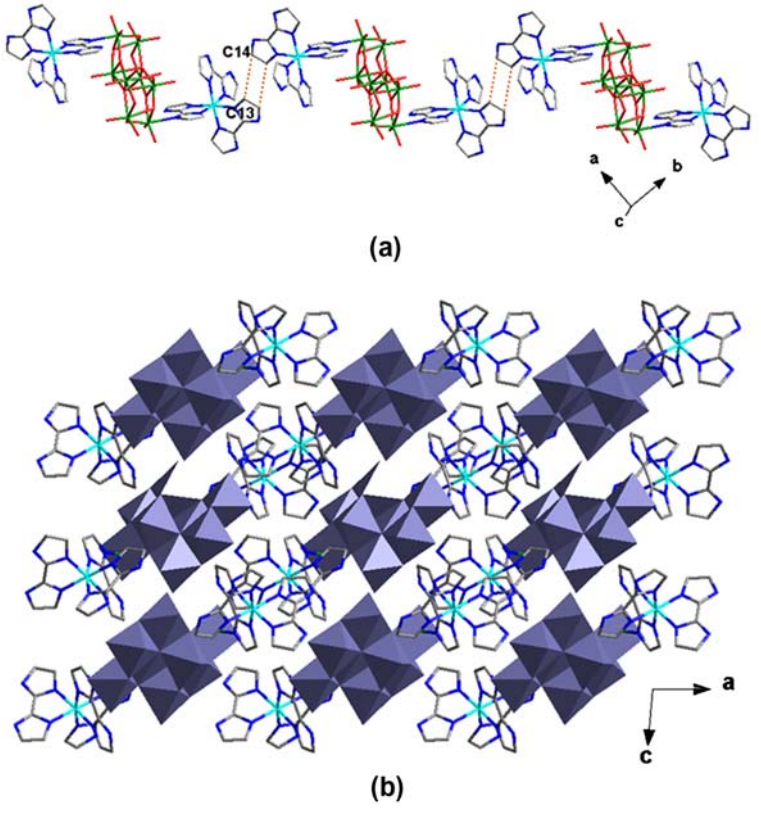

Figure 3. (a) The π…π stacking interactions induce the supramolecular 1D chain of **1**. (b) The 3D supramolecular structure of **1**.

Between these two-supporting anions, there are π…π stacking interactions, such as C13–C14 = 3.606 Å, inducing a supramolecular 1-D chain (figure 3(a)). Waters of crystallization between these supramolecular chains have hydrogen-bonding interactions with γ-Mo_8 and H_2biim. Thus, a supramolecular 3-D structure is formed (figure 3(b)).

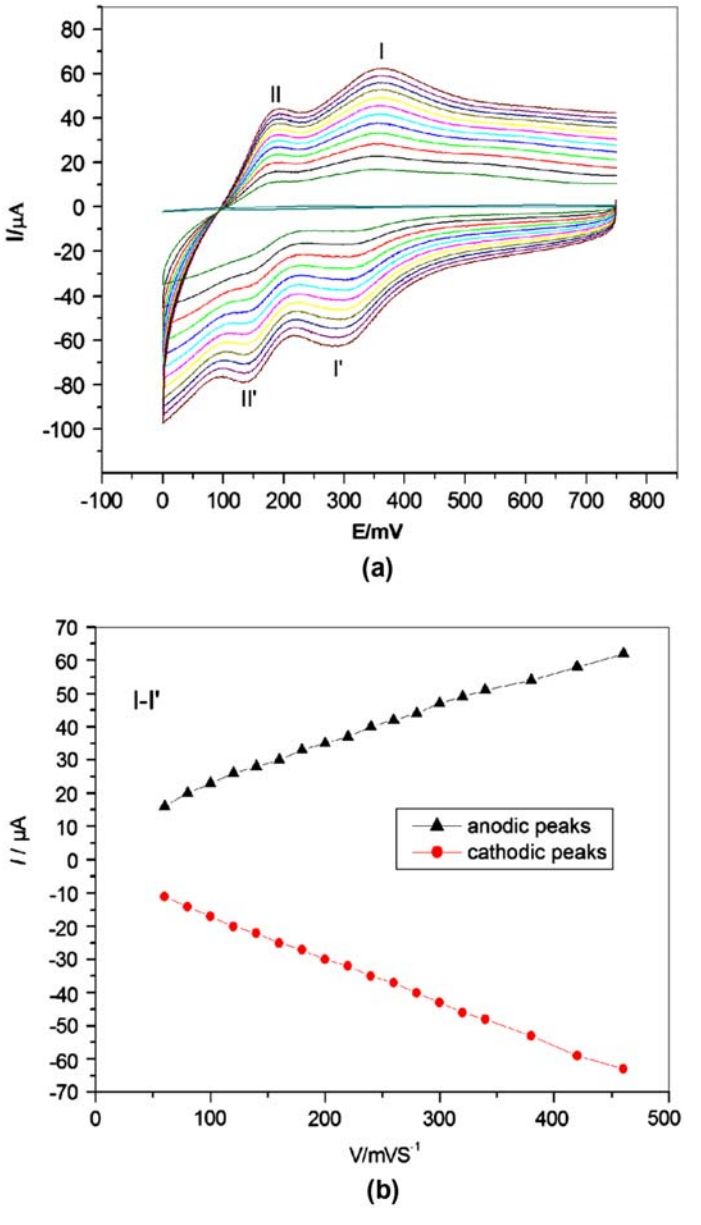

Figure 4. (a) Cyclic voltammograms of a bare CPE at scan rate of 80 mV s^{-1} (inner) and **1**–CPE in 1 M H_2SO_4 at different scan rates (from inner to outer: 60, 100, 140, 180, 220, 240, 280, 320, 360, 400, 440 and 480 mV s^{-1}). (b) Plots of the anodic and the cathodic peak I–I′ current against v.

3.3. *IR spectrum*

The IR spectrum of **1** is shown in figure S1. Characteristic bands at 941, 855, 775, and 684 cm^{-1} are attributed to the $\nu(Mo=O_t)$ and $\nu(Mo–O–Mo)$, respectively. Bands at 1635–1106 cm^{-1} are attributed to H_2biim.

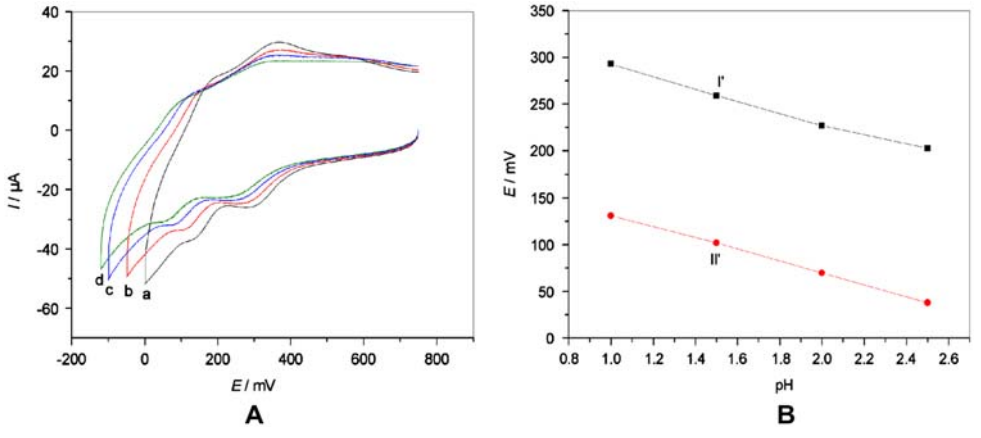

Figure 5. (A) Cyclic voltammograms for the **1**–CPE in $H_2SO_4 + Na_2SO_4$ solutions with different pH: (a) 1.0; (b) 1.5; (c) 2.0; (d) 2.5. (B) The relationship of peak potential and pH. Scan rate: 100 mV s^{-1}.

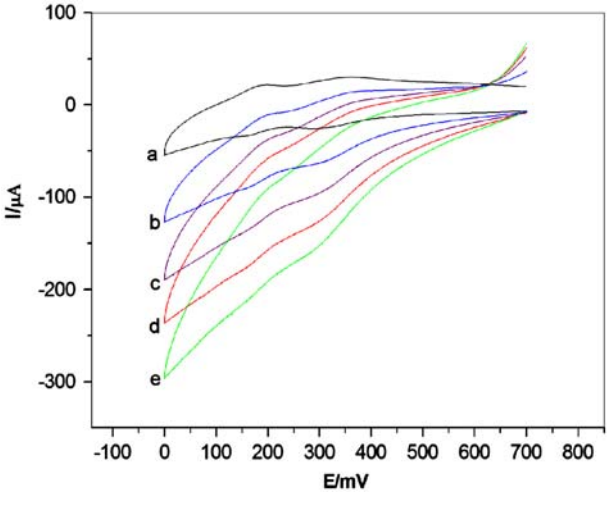

Figure 6. Cyclic voltammograms of the **1**–CPE in 1 M H_2SO_4 containing 0(a); 2(b); 4(c); 6(d); 8(e) mM KNO_2. Scan rate: 150 mV s^{-1}.

3.4. *Thermal analysis*

The TGA experiment was performed under N_2 with a heating rate of 10 °C min^{-1} from 20 to 600 °C and its plot is shown in figure S2. The TG curve of **1** shows two distinct weight loss steps. The first weight loss step below 240 °C corresponds to loss of waters 6.39% (calc. 6.37%) and the second can be attributed to the loss of organic molecules 35.23% (calc. 35.51%) from 240 to 600 °C.

3.5. *Cyclic voltammetry*

The CPE is the optimal choice to study the electrochemical properties of **1** which is insoluble in water and common organic solvents. The cyclic voltammograms for **1**–CPE in

1 M H_2SO_4 aqueous solution at different scan rates are presented in figure 4(a). Two reversible redox peaks appear in the potential range 750–0 mV with half-wave potentials $E_{1/2} = (E_{pa} + E_{pc})/2$ of + 337 (I–I′) and + 164 (II–II′) mV (scan rate: 80 mV s^{-1}), respectively, which can be ascribed to redox of Mo centers. The peak potentials change gradually with scan rates from 60 to 480 mV s^{-1}: the cathodic peak potentials shift negative and the corresponding anodic peak potentials positive with increasing scan rates. When the scan rates are lower than 500 mV s^{-1}, the peak currents are proportional to the scan rates, which indicates that the redox process of **1**–CPE is surface-confined (figure 4(b)). The redox ability of the parent $[Mo_8O_{26}]^{4-}$ can be maintained in the hybrid solids promising an application of this kind of inorganic–organic hybrid materials in electrochemistry.

3.6. *pH-dependent electrochemical behavior of 1–CPE*

The pH of the supporting electrolyte has a remarkable effect on the electrochemical behavior of **1**–CPE in $H_2SO_4 + Na_2SO_4$ aqueous solutions. As can be seen from figure 5(a), following the increase of pH, both waves shift to more negative potentials and the peak currents decrease. Plots of peak potentials of two redox waves versus pH for **1**–CPE show good linearity from 1.0 to 2.5 (see figure 5(b)). Slopes of the pH range are −60, −62, and −75 mV pH^{-1}, corresponding to the addition of approximately two protons [18].

3.7. *Electrocatalytic activity of 1–CPE*

Figure 6 shows cyclic voltammograms for electrocatalytic reduction of nitrite at **1**–CPE in 1 M H_2SO_4 aqueous solution. The **1**–CPE displays an electrocatalytic activity towards reduction of nitrite. At **1**–CPE, with the addition of nitrite, the two reduction peak currents increase gradually while the corresponding oxidation peak currents gradually decrease. This result suggests that **1** exhibits good electrocatalytic activity to reduce nitrite.

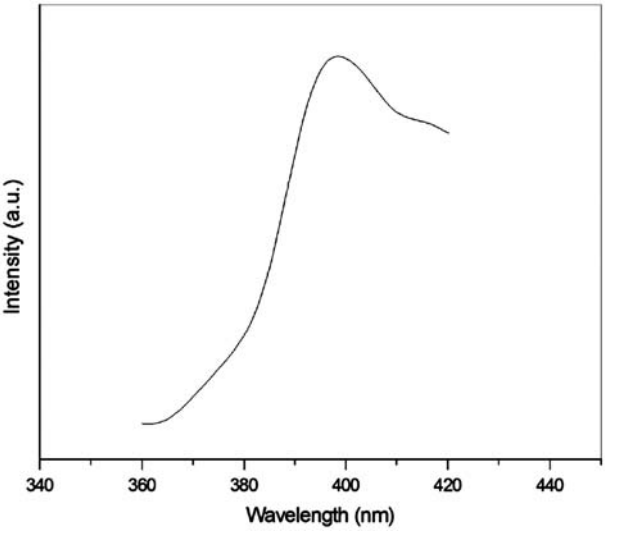

Figure 7. Solid-state emission spectrum of **1** at room temperature.

3.8. *Photoluminescence property*

Photoluminescence spectra of powder samples of **1** and H_2biim at room temperature are shown in figure 7 and figure S3. **1** exhibits photoluminescence with an emission maximum at *ca.* 398 nm upon excitation at *ca.* 320 nm. The emission peaks are assigned to the intral-igand n–π^* charge transfer [19]. By contrast, H_2biim exhibits a strong peak at 366 nm in the same excitation, which may be due to formation of metal-ligand coordination.

4. Conclusions

A new octamolybdate-based **1** has been synthesized under hydrothermal conditions. In **1**, the octamolybdate shows an γ isomer, exposing two [MoO_5] units. Three H_2biim chelate one Zn to form a cationic $[Zn(H_2biim)_2(Hbiim)]^+$ subunit, two subunits link one octamolybdate through Mo–N bonds, forming a two-supporting anion. The two exposed [MoO_5] units of γ-Mo_8 offer two Mo to coordinate with N donors of the cationic subunit. This work enriches examples of isopolymolybdate-based compounds containing Mo–N bonds. Further study on other new organic ligands is underway for exploring Mo–N containing structures.

Acknowledgments

We are thankful for the financial support from the National Natural Science Foundation of China (Nos. 21101015 and 21171025), New Century Excellent Talents in University (NCET-10-0853) and Natural Science Foundation (201102003) and Doctoral Initiation Project (No. 20111147) of Liaoning Province.

References

[1] (a) B.S. Bassil, M. Ibrahim, R. Al-Oweini, M. Asano, Z.X. Wang, J. Tol, N.S. Dalal, K.-Y. Choi, R.N. Biboum, B. Keita, L. Nadjo, U. Kortz. *Angew. Chem., Int. Ed.*, **50**, 5961 (2011); (b) F.J. Ma, S.X. Liu, C.Y. Sun, D.D. Liang, G.J. Ren, F. Wei, Y.G. Chen, Z.M. Su. *J. Am. Chem. Soc.*, **133**, 4178 (2011); (c) D.Y. Du, J.S. Qin, Y.G. Li, S.L. Li, Y.Q. Lan, X.L. Wang, K.Z. Shao, Z.M. Su, E.B. Wang. *Chem. Commun.*, **47**, 2832 (2011).

[2] (a) M. Nyman, C.R. Powers, F. Bonhomme, T.M. Alam, E.J. Maginn, D.T. Hobbs. *Chem. Mater.*, **20**, 2513 (2008); (b) Y.L. Zhong, W. Ng, J.X. Yang, K.P. Loh. *J. Am. Chem. Soc.*, **131**, 18293 (2009); (c) S.X. Guo, A.W.A. Mariotti, C. Schlipf, A.M. Bond, A.G. Wedd. *Inorg. Chem.*, **45**, 8563 (2006).

[3] (a) C.Y. Sun, S.X. Liu, D.D. Liang, K.Z. Shao, Y.H. Ren, Z.M. Su. *J. Am. Chem. Soc.*, **131**, 1883 (2009); (b) H.J. Pang, J. Peng, C.J. Zhang, Y.G. Li, P.P. Zhang, H.Y. Ma, Z.M. Su. *Chem. Commun.*, **46**, 5097 (2010); (c) S.T. Zheng, J. Zhang, J.M. Clemente-Juan, D.Q. Yuan, G.Y. Yang. *Angew. Chem., Int. Ed.*, **48**, 7176 (2009).

[4] (a) X.L. Wang, C. Qin, E.B. Wang, Z.M. Su, Y.G. Li, L. Xu. *Angew. Chem., Int. Ed.*, **45**, 7411 (2006); (b) B. Liu, Z.T. Yu, J. Yang, W. Hua, Y.Y. Liu, J.F. Ma. *Inorg. Chem.*, **50**, 8967 (2011).

[5] (a) H. Abbas, C. Streb, A.L. Pickering, A.R. Neil, D.L. Long, L. Cronin. *Cryst. Growth Des.*, **8**, 635 (2008); (b) Y.Q. Lan, S.L. Li, X.L. Wang, K.Z. Shao, Z.M. Su, E.B. Wang. *Inorg. Chem.*, **47**, 529 (2008).

[6] H.Y. Zang, K. Tan, W. Guan, S.L. Li, G.S. Yang, K.Z. Shao, L.K. Yan, Z.M. Su. *Cryst. Eng. Comm.*, **12**, 3684 (2010).

[7] (a) M.X. Yang, L.J. Chen, S. Lin, X.H. Chen, H. Huang. *Dalton Trans.*, **40**, 1866 (2011); (b) H.Y. Zang, Y. Q. Lan, G.S. Yang, X.L. Wang, K.Z. Shao, G.J. Xu, Z.M. Su. *Cryst. Eng. Comm.*, **12**, 434 (2010).

[8] (a) A. Kumar, V. Singh, A.N. Gupta, M.K. Yadav, V. Kumar, N. Singh. *J. Coord. Chem.*, **65**, 431 (2012); (b) L.M. Fan, D.C. Li, P.H. Wei, J.M. Dou, X.T. Zhang. *J. Coord. Chem.*, **63**, 4226 (2010); (c) M.X. Li, G. L. Guo, J.Y. Niu. *J. Coord. Chem.*, **61**, 3860 (2008); (d) C.L. Wang, S.X. Liu, C.Y. Sun, L.H. Xie. *J. Coord. Chem.*, **61**, 891 (2008); (e) C.H. Tian, Z.G. Sun, L.C. Zhang, H.D. Liang, Z.M. Zhu, W.S. You, Y.P. Gu. *J. Coord. Chem.*, **60**, 985 (2007).

[9] M.X. Li, H.L. Chen, J.P. Geng, X. He, M. Shao, S.R. Zhu, Z.X. Wang. *Cryst. Eng. Comm.*, **13**, 1687 (2011).
[10] (a) H.Y. Zang, Y.Q. Lan, S.L. Li, G.S. Yang, K.Z. Shao, X.L. Wang, L.K. Yan, Z.M. Su. *Dalton Trans.*, **40**, 3176 (2011); (b) X.L. Wang, J. Li, A.X. Tian, G.C. Liu, Q. Gao, H.Y. Lin, D. Zhao. *CrystEngComm.*, **13**, 2194 (2011).
[11] A.X. Tian, X.J. Liu, J. Ying, D.X. Zhu, X.L. Wang, J. Peng. *Cryst. Eng. Comm.*, **13**, 6680 (2011).
[12] G.M. Sheldrick. *Acta Crystallogr., Sect. A*, **64**, 112 (2008).
[13] K. Pavani, A. Ramanan. *Eur. J. Inorg. Chem.*, **3080**, (2005).
[14] (a) J.Q. Sha, J. Peng, Y.Q. Lan, Z.M. Su, H.J. Pang, A.X. Tian, P.P. Zhang, M. Zhu. *Inorg. Chem.*, **47**, 5145 (2008). (b) A.X. Tian, Z.G. Han, J. Peng, J.Q. Sha, Y.L. Zhao, H.J. Pang, P.P. Zhang, M. Zhu. *Solid State Sci.*, **10**, 1352 (2008). (c) A.X. Tian, J. Ying, J. Peng, J.Q. Sha, H.J. Pang, P.P. Zhang, Y. Chen, M. Zhu, Z. M. Su. *Inorg. Chem.*, **48**, 100 (2009).
[15] (a) J.Q. Sha, Y.H. Zhang, L.Y. Liang, H.B. Qiu, M.Y. Liu. *J. Coord. Chem.*, **65**, 3264 (2012). (b) L.M. Fan, D.C. Li, P.H. Wei, G.Z. Liu, X.T. Zhang, J.M. Du. *J. Coord. Chem.*, **64**, 2531 (2011).
[16] I.D. Brown, D. Altermatt. *Acta Crystallogr., Sect. B*, 41, 244 (1985).
[17] Z.Y. Shi, J. Peng, C.J. Gómez-García, S. Benmansour, X.J. Gu. *J. Solid State Chem.*, **179**, 253 (2006).
[18] (a) N. Fay, E. Dempsey, T. McCormac. *J. Electroanal. Chem.*, **574**, 359 (2005). (b) N. Fay, E. Dempsey, A. Kennedy, T. McCormac. *J. Electroanal. Chem.*, **63**, 556 (2003).
[19] X.L. Wang, Y.F. Bi, B.K. Chen, H.Y. Lin, G.C. Liu. *Inorg. Chem.*, **47**, 2442 (2008).